Inverse order-disorder transition of charge stripes

Shu-Han Lee, Yen-Chung Lai, and Chao-Hung Du*

Department of Physics, Tamkang University,

Tamsui Dist., New Taipei City 25137, Taiwan

Alexander F. Siegenfeld

Department of Physics, Massachusetts Institute of Technology,

77 Massachusetts Avenue, Cambridge, MA 02139-4307

Ying-Jer Kao†

Advanced Center for Theoretical Science and Department of Physics,

National Taiwan University, No. 1, Sec. 4,

Roosevelt Rd. Taipei, 10607, Taiwan

Peter D. Hatton

Department of Physics, Durham University, Durham DH1 3LE, UK

D. Prabhakaran

Department of Physics, University of Oxford,

Clarendon Laboratory, Parks Road, OX1 3PU, UK

Yixi Su

Juelich Centre for Neutron Science JCNS, Forschungszentrum Juelich GmbH,

Outstation at MLZ, D-85747, Garching, Germany

Di-Jing Huang

National Synchrotron Radiation Research Center,

101 Hsin-Ann Road, Hsinchu 30076, Taiwan

(Dated: October 20, 2015)

Abstract

We report an unusual transition behavior of charge stripes in $La_{1.67}Sr_{0.33}NiO_4$ using x-ray scattering. The segregated holes in $La_{1.67}Sr_{0.33}NiO_4$ are observed to form anisotropic stripes in the $a\times b$ plane of the crystal space below the transition temperature $T \simeq 238$ K, and at the same time, display an unusual inverse order-disorder transition along the c-axis. Using a phenomenological Landau theory, we show that this inverse transition is due to the interlayer coupling between the charge and spin orders. This discovery points to the importance of the interlayer correlations in the strongly correlated electrons system.

Doped Mott insulators have served as a rich playground for strongly correlated electron systems, yet the physics is still not fully comprehended. The complexity results from the interplay between competing orders such as charge, spin, orbital, and lattice, and the strong quantum fluctuations [1]. In the model system of high-T_c superconductor La_2CuO_4, substitution of La with Sr or Ba induces segregated holes that form unidirectional self-organized electronic stripes in the $a\times b$ plane of the crystal space [2]. Experimentally, such a phenomenon has been observed in neutron, x-ray, and electron diffractions, and it is shown that transport behavior depends strongly on the hole concentration [3, 4]. These ordered electronic phases are understood to arise due to the Coulomb-frustrated separation of electronic domains at the nanoscale [5, 6]. In these phases, there exist locally Mott insulating regions with magnetic (spin) order, separated by more metallic regions with higher concentrations of doped holes. Taking the in-plane fluctuations into consideration, these ordered charges could form the exotic electronic liquid-crystal phases [7, 8]. This intralayer coupling between the ordered charges and spins has been widely discussed and observed in Cu- and Fe-based superconductors [9–12]. It is natural to ask what role the *interlayer* coupling between the charge and spin orders in different planes plays in these systems [13, 14].

Using x-ray scattering measurements on single-crystal samples of $La_{2-x}Sr_xNiO_4$ (LSNO), we report an unusual inverse order-disorder transition due to the interlayer coupling of the in-plane charges and spins. It is well established that there can exist both smectic and striped-liquid phases of in-plane charge and spin ordering in LSNO [15–18]. LSNO has a tetragonal structure (Fig. 1*a*), and is isostructural with the superconducting cuprate LSCO. Both LSNO and LSCO are antiferromagnetic (AFM) Mott insulators in the absence of hole doping. While LSCO becomes a high-T_c superconductor for small amounts of hole doping, LSNO remains insulating for doping levels of up to 90% [19].

In LSNO the doped holes condense, leaving, within each 2D NiO layer, an alternating pattern of AFM domains (spin stripes) separated by charge stripes (Fig.1*b*). In the reciprocal space of the tetragonal crystal structure ($F4/mmm$), the stripes lead to charge and spin satellite reflections with wavevectors of $\mathbf{Q}_{\rm CO} = (H \pm 2\epsilon\ 0\ L_1)$ and $\mathbf{Q}_{\rm SO} = (H \pm \epsilon\ 0\ L_2)$, where H and L_2 are integers, L_1 is odd, and ϵ is determined by hole concentration with $\epsilon \sim x$. For $La_{1.67}Sr_{0.33}NiO_4$ ($x = 1/3$), the charge and spin orders are commensurate with the lattice, and satellite reflections from the charge stripes superimpose on those from the spin stripes (Fig. 1*c*), a condition that proves essential for the inverse transition of the interlayer charge order.

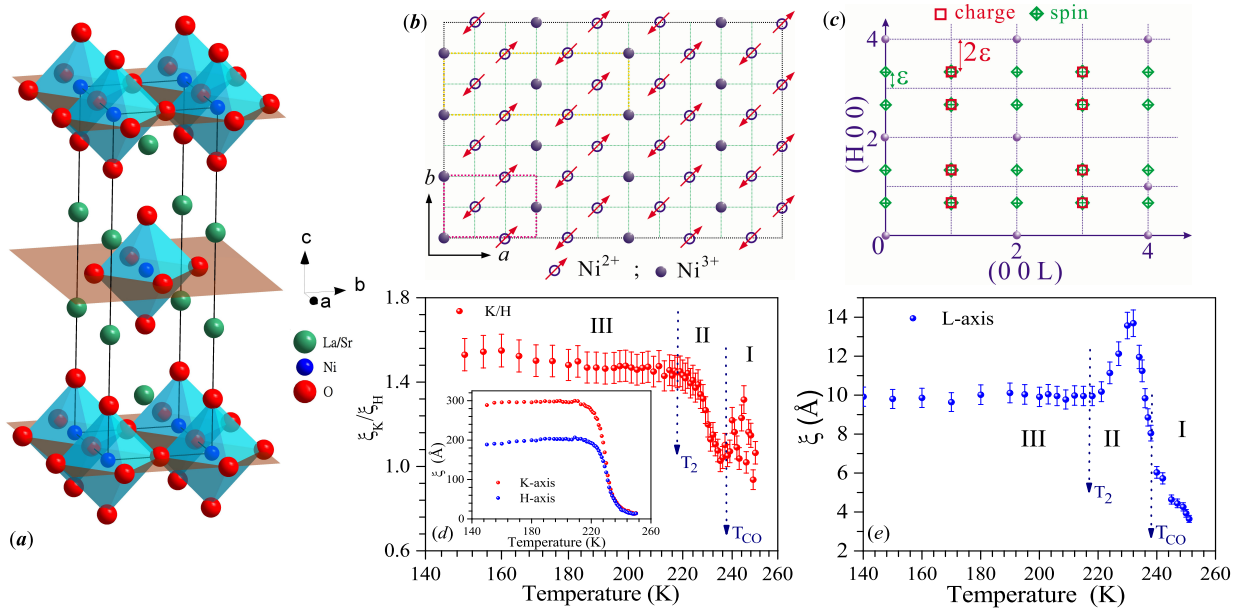

FIG. 1. (Color online) Schematic views of crystal structure and charge stripes, and the evolution of correlation lengths of charge stripes as a function of temperature. (a) The crystal structure of $La_{1.67}Sr_{0.33}NiO_4$. (b) Schematic view of charge and spin stripes in $La_{1.67}Sr_{0.33}NiO_4$ in NiO_2 planes of the tetragonal unit cell. The arrows represent the Ni^{2+} ions, and solid circles are the holes. Yellow and red boxes indicate the size of the spin and charge modulations. (c) The satellite reflections of charge and spin stripes in the (H 0 L) plane of reciprocal space. Since the incommensurability ϵ $\sim$ 0.33, charge reflection satellites superimpose on spin reflections. (d) Temperature evolution of the ratio of the correlation lengths along the K and H directions. The data can be divided into 3 regions with two transition temperatures of T_{CO} ($\sim$238 K) and T_2 ($\sim$218 K), as marked I, II, and III. The inset shows the evolution of the correlation lengths of the charge stripes along the H and K directions as a function of temperature. (e) Evolution of the correlation length along the L-direction as a function of temperature. As can be seen, there is an inverse order-disorder transition at around 230 K. The correlation lengths were extracted from the inverse of FWHM (full width at half maximum) of the charge ordering reflections.

For this study, high quality single crystals of $La_{1-x}Sr_xNiO_4$, x= 0.225, 0.33, and 0.4, were grown by the floating zone method at University of Oxford. The crystals were characterized and orientated using conductivity measurements and an in-house x-ray diffractometer, and the surface was polished using 0.1 μ diamond paste. The values of x were further confirmed by checking the transition temperatures of charge modulation using synchrotron x-ray scat-

tering. Synchrotron x-ray scattering experiments were performed on the beamlines BL07 and SP12B1 of NSRRC (Taiwan) and SP8 (Japan). The incident x-ray energy was selected to be 10 keV. The sample was mounted on a closed-cycle cryostat on a multi-circle diffractometer. A single crystal of LiF (0 0 1) was used as an analyzer to define the scattered x-rays from the sample. The experimental resolution function was determined to be $\epsilon_H^{-1} \sim 0.0019$ Å^{-1}, $\epsilon_K^{-1} \sim 0.001$ Å^{-1}, and $\epsilon_L^{-1} \sim 0.015$ Å^{-1} as measured on the Bragg peak (4 0 0) near the charge ordering peaks at $T = 140$ K, with the sample mosaic width $\sim 0.02°$. For the study of spin stripes, resonant soft X-ray scattering measurements were performed on the beamline BL05B3 of NSRRC. The measurements were performed to scan the spin stripe reflection (0.66 0 0) through the L_3 edge of Ni.

Figure 1*d* shows, as a function of temperature, the ratio of the charge correlation lengths along the H and K directions in the reciprocal space. The data can be divided into 3 regions with two transition temperatures of T_{CO} (∼238 K) and T_2 (∼218 K), as marked I, II, and III. In regime I ($T >$ 238K), the segregated charges are in an disordered and isotropic state. Upon cooling, the segregated charges form anisotropic charge stripes , and the anisotropy displays a temperature dependent behavior in regime II (218 K$< T <$ 238 K). Finally, the anisotropy reaches nearly constant in regime III (below T_2). The detailed peak profiles can be seen in Fig. 1 and 2 of the supplementary material. LSNO has been known not to have any lattice distortions at low temperatures [20, 21], so this anisotropic behaviour is a result of an intrinsic charge modulation.

The unusual data comes from the measurements taken along the L-direction in the reciprocal space, shown in Fig. 1*e*. Cooling from high temperatures, the charge correlation starts to build up significantly along the c-axis of the crystal at around $T = 238$ K, and the charge correlation lengths start to increase from $\xi =$ ∼6 Å to 14 Å as temperature is cooled down to $T = 230$ K. At this temperature, the interlayer charge correlation spans over two NiO layers and it seems that a full 3D ordering will eventually develop if there are not existence of any imperfections in the crystal [22]. However, when the temperature is further decreased, the interlayer charge correlation starts to decrease, rather than increase, and the inverse order-disorder transition occurs. Finally, the interlayer charge correlation length reaches $\xi =$ ∼10 Å below $T =$ 218 K, where both the charge and spin stripes are well established. We realize, for the c-axis correlation length at low temperatures, that it exists a discrepancy between the current data and the reported result [22]. This difference could be due to the different sample treatments as that reported by Hücker *et. al.* [21].

Attention was also paid to study the thermal effect of charge stripes. Under different thermal sequences, (as described in Supplementary), charge stripes show a thermal hysteresis behavior around the transition (see Supplementary Fig. 4), suggesting that charge stripes are in a non-equilibrium state just below the transition temperature.

Experiments were also conducted to measure the spin stripes using resonant soft x-ray diffraction. Figure 2*a* shows the temperature dependence of the integrates intensity of the charge stripe reflection (4.66 0 3) and spin stripe reflection (0.66 0 0). It evidences that charge stripes undergoes a second order phase transition. This is consistent with our previous report of a quenched disordered charge stripes [22]. According to our model, this quenched disordered state is the consequence of the interplay between charges and spins. It is worth notice that the very weak spin ordering reflection is still observable at temperature of 230 K by means of resonant soft x-ray diffraction at Ni L_3 edge. This behavior is in accord with the reported result by Anissimova *et. al.* using neutron scattering, and suggesting a strong coupling between the charge and spin stripes [17]. Figure 2*b* shows the temperature evolution of the peak profile of a spin stripe satellite reflection at (0.66 0 0) measured along the H direction, which serves as a measure of in-plane spin order, and of a charge stripe satellite reflection at (4.66 0 3) along the L direction, which serves as a measure of interlayer charge correlation. Although the spin stripe transition occurs at a temperature of around $190K$, the satellite reflection persists up to temperatures as high as $230K$, indicating a dynamic spin fluctuations at high temperatures [17, 18]. The onset of the interlayer charge order suppression coincides with the appearance of the in-plane spin stripe order, suggesting that the in-plane spin stripe order plays an important role in the inverse transition of the interlayer charge order.

In order to model the observed behavior in LSNO, we construct a Landau theory for the spin and charge stripe orders for a bilayer system with 2D layers. For simplicity we assume that the spin and charge order in each layer can be described by single complex Fourier coefficients and that the spin order is collinear; thus the order parameters can be written as $\mathbf{S}_i = |S_i|e^{i(\phi_i+\mathbf{r}_i\cdot\mathbf{q}_i^S)}\hat{\mathbf{m}}_i$ and $\rho_i = |\rho_i|e^{i(\theta_i+\mathbf{r}_i\cdot\mathbf{q}_i^\rho)}$, where $\mathbf{q}_i^S$ is measured relative to the in-plane antiferromagnetic ordering vector $\mathbf{Q} = (1, 0, 0)$ and $i \in \{1, 2\}$ denotes the layer index. We take $2\mathbf{q}_1^S = 2\mathbf{q}_2^S = \mathbf{q}_1^\rho = \mathbf{q}_2^\rho$, so as to allow coupling between the order parameters within and between layers[23].

Starting from the most general Landau free energy for a single layer that includes all symmetry allowed terms up to the fourth order and then applying a few simplifications

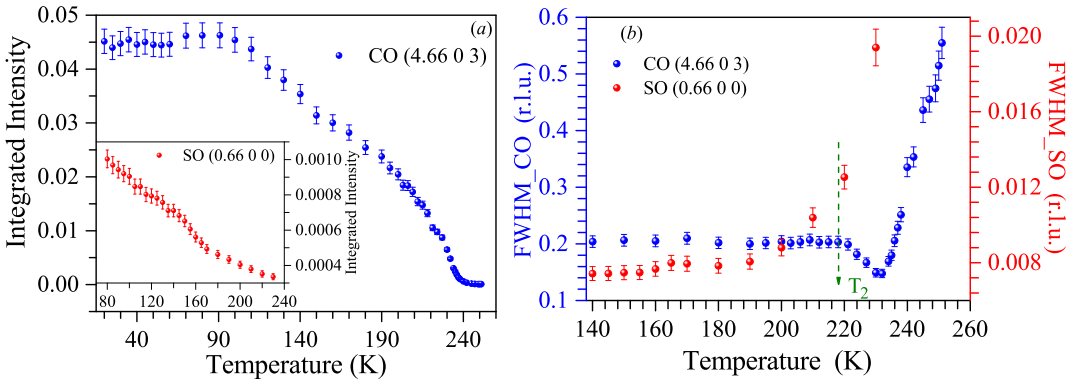

FIG. 2. (Color online) Interplay between charge and spin stripes. (*a*) Temperature dependence of the integrated intensity for charge ordering reflection (CO) and spin ordering reflection (SO). (*b*) Evolution of peak width as a function of temperature for the CO reflection (4.66 0 3) [blue dots] and the SO reflection (0.66 0 0) [red dots]. The charge reflection was measured along the *L*-direction using hard x-rays, and the spin reflection was measured along the *H*-direction by resonant soft x-ray diffraction. It can be seen that the spin stripe order exists up to ∼230 K. The onset of the interlayer correlation suppression coincides with the onset of the in-plane spin order, indicating a close relationship between the two.

yields [23]

$$F_i = \frac{1}{2}r_s|S_i|^2 + |S_i|^4 + \frac{1}{2}r_\rho|\rho_i|^2 + |\rho_i|^4 + \lambda_1|S_i|^2|\rho_i|\cos(2\phi_i - \theta_i). \tag{1}$$

We take the free energy due to the interlayer coupling to be

$$\begin{aligned} F_c =& \lambda_\rho(\rho_1\rho_2^* + c.c.) + \lambda_2([(\mathbf{S_1}\cdot\mathbf{S_1})\rho_2^* + (\mathbf{S_2}\cdot\mathbf{S_2})\rho_1^*] + c.c.) \\ =& 2\lambda_\rho|\rho_1||\rho_2|\cos(\theta_1 - \theta_2) + 2\lambda_2\left[|S_2|^2|\rho_1|\cos(2\phi_2 - \theta_1)\right. \\ &\left. + |S_1|^2|\rho_2|\cos(2\phi_1 - \theta_2)\right], \end{aligned} \tag{2}$$

where the λ_ρ term is due to Coulomb repulsion between layers and the λ_2 term is due to the fact that the holes are to some extent delocalized between layers.

The total free energy is $F = F_1 + F_2 + F_c$, but considering that intralayer interactions are far stronger than interlayer ones, the approximate values of $|S_i|$, $|\rho_i|$, and $2\phi_i - \theta_i$ can be determined by examining only the single-layer free energy, resulting in $|S_1| = |S_2| \equiv S$ and $|\rho_1| = |\rho_2| \equiv \rho$, and leaving only the interlayer phase shift of $\alpha \equiv \theta_1 - \theta_2$ to be determined by the interlayer coupling. Minimizing the intralayer free energies requires $\cos(2\phi_i - \theta_i) = -1$,

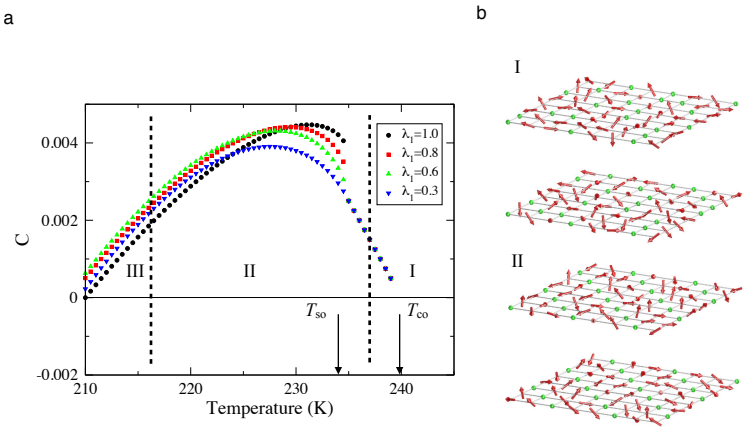

FIG. 3. (Color online) Bilayer correlations from the Landau theory, and spin and charge configurations in different phases. (a) Plot of C, the stiffness of the interlayer phase shift defined in the text, as a function of temperature for several intra-layer charge-spin coupling constants. (b) Real-space configurations of the states in different temperature regimes. In the high temperature regime I, there exists no or very weak in-plane charge order and the correlation between layers is small. In regime II, charge stripe order develops while the spins remain disordered. The charge stripes between layers tend to be anti-phase to minimize the Coulomb repulsion between layers.

since λ_1 is positive[23], and so we obtain $F_c = 2\rho(\lambda_\rho \rho - 2\lambda_2 S^2)\cos\alpha$. A good measure of the strength of the interlayer coupling is the stiffness of the phase shift $C \equiv \frac{\partial^2 F_c}{\partial \alpha^2} = |2\rho(\lambda_\rho \rho - 2\lambda_2 S^2)|$ at equilibrium. For a large C, the phase shift between layers of the charge stripes is harder to fluctuate and the phase angles tend to be anti-phase to minimize the free energy. On the other hand, for small C, the phase shift between layers becomes less rigid and allows for more fluctuations, leading to a reduction of interlayer correlation. It is now clear why the interlayer correlations at first increase and then decrease as the temperature T is lowered: at high temperatures, $\rho = S = 0$ so there are no interlayer correlations. Charge order appears first and so C at first increases, but at lower temperatures spin order also appears thus causing C to then decrease. At still lower temperatures we expect the Landau theory to no longer accurately model the system.

Giving r_ρ and r_s linear temperature dependence and taking λ_1 to be temperature independent, C will always, after an initial increase, decrease as temperature is lowered, regardless of the exact values of the parameters. As shown in Fig. $3a$, C behaves similarly to the interlayer correlation length (Fig. $2d$) for temperatures not too far from the onset of the stripe orders. Figure 3b shows the real-space configurations for regime I and II. In regime

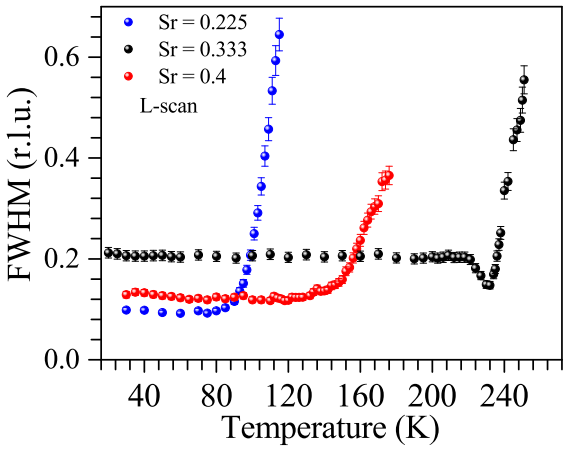

FIG. 4. (Color online) Peak widths of charge stripes with different hole concentrations. The data were taken from single crystals ($La_{2-x}Sr_xNiO_4$) with different hole concentrations, i.e., $x = 0.225$, 0.33, and 0.4. As can be seen, the inverse order-disorder transition occurs only for $x = 0.33$.

I, there exists no or very weak in-plane charge order and the correlation between layers is small. In regime II, charge stripe order develops while the spins remain disordered. Out-of-plane charge correlation develops to minimize the Coulomb repulsion. In regime III, the spin order develops and the out-of-plane charge correlation is suppressed and we expect the system goes into a three-layer stacking as described in Ref. [21].

Intuitively, this curious rise and fall of interlayer correlation is a result of two competing interactions [24]. The interlayer charge-charge coupling favors the stripes in different layers to be out of phase because the charge stripes repel each other, while the interlayer charge-spin coupling favors in-phase stripes because the formation of in-plane spin modulation causes the dissipation of kinetic energy of the electrons. In-plane charge order appears first, resulting in the buildup of an out-of-phase interlayer charge correlation, but as the in-plane spin stripe order starts to develop, the interlayer charge order is suppressed.

Figure 4 shows the measurements at doping concentrations $x = 0.225, 0.33$, and 0.4; only at $x = 0.33$ does the inverse transition occur. This phenomenon adds to the list of anomalies for $La_{1.67}Sr_{0.33}NiO_4$ due to the commensurate pinning of the charges to the Ni lattice at $x = 0.33$ [20, 25–28]. For $x \neq 0.33$, topological defects, such as dislocations and kinks, can easily proliferate to destabilize the in-plane charge stripe order [29, 30]. This also weakens the phase-dependent interlayer charge-spin couplings in Eq. (2); as a result, there are no competing interlayer interactions to cause the inverse transition of the interlayer correlation.

Our work points to the importance of the interlayer coupling in LSNO. However, it is

worth notice that, using x-ray scattering on the family compounds $Pr_{1-x}Sr_xNiO_4$ (PSNO) and $Nd_{1-x}Sr_xNiO_4$ (NSNO), H*ücker et.al.* [21] points out that a stacking fault of NiO_2 layers can induce a minimum of the correlation length of charge stripes along the c-axis just below the transition temperature. Compared with PNSO and NSNO, LSNO shows no orthorhombic strain, so the stacking fault is expected to have the less effect on governing the interlayer coupling, however, the similar behavior for spin stripes would be expected if the stacking fault of NiO_2 layers is the major driving face for the formation of inverse order-disorder. Interlayer Coulomb interaction has been argued to be crucial in understanding an anomalous shrinking of the c/a lattice parameter ratio that correlates with T_{CO} in $La_{1.67}Sr_{0.33}NiO_4$ [20], as well as the existence of fluctuating charge stripes that persist to high temperatures [20, 22]. In particular, the inverse order-disorder transition of the interlayer charge order observed in this work may provide a new direction to understand the dominance of the dynamical stripes in cuperates. Further extension of the current work to study the dynamical interlayer correlations in $La_{1.67}Sr_{0.33}NiO_4$ [20, 31] and its sister compound $La_{1.67}Sr_{0.33}CoO_4$ [32, 33] may help to elucidate the unusual transport behavior caused by the charge/spin stripes in the transition metal oxides.

We acknowledge many stimulating discussions with Profs. Cheng-Hsuan Chen and Bruce Gaulin. We are grateful to MOST in Taiwan for the financial support through grant Nos. 99-2112-M-032-005- MY3 and 102-2112-M-032-004-MY3 (CHD), 102-2112-M-002 -003 -MY3 (YJK).

APPENDIX: CHARGE AND MAGNETIC CORRELATIONS

Synchrotron X-ray scattering experiments were carried out on the beamlines BL07 and SP12B1 of NSRRC, Taiwan. The sample was mounted on a closed-cycle cryostat mounted on a multi-circle diffractometer, which allows the scans to be performed along any of the reciprocal space crystallographic axes, $H(=2\pi/a)$, $K(=2\pi/b)$, and $L(=2\pi/c)$. Throughout this study for $La_{5/3}Sr_{1/3}NiO_4$, a tetragonal unit cell with lattice parameters of $a = b = 5.4145$ Å $= 2\sqrt{2}d_{Ni-O}$ and $c = 12.715$ Å was used to index the reflections. There was no realignment of the crystal during the measurements because $La_{5/3}Sr_{1/3}NiO_4$ does not display any structural phase transitions at low temperatures [20]. The incident x-ray energy was set to 10 keV by a pair of high quality single crystals of Si(1 1 1), and a LiF crystal was used in an analyzer to define the scattered x-rays from the sample. The experimental resolution

function was determined to be $\epsilon_H^{-1} \sim 0.0019$ Å^{-1}, $\epsilon_K^{-1} \sim 0.001$ Å^{-1}, and $\epsilon_L^{-1} \sim 0.015$ Å^{-1} as measured on the Bragg peak (4 0 0), which is near the charge ordering peaks measured at $T = 140$ K, and the sample mosaic width was found to be $\sim 0.02°$. The peak profiles of the Bragg reflection (4 0 0) were monitored throughout the measurements and showed no changes. The correlation lengths of the charge stripe reflections were extracted from their measured peak profiles convoluted with the resolution functions, and the error bars shown in this study were taken from the square-root of the data points. Measurements were taken as a function of temperature through the Bragg peak and charge stripe satellites along the crystallographic axes of H, K, and L in the reciprocal space.

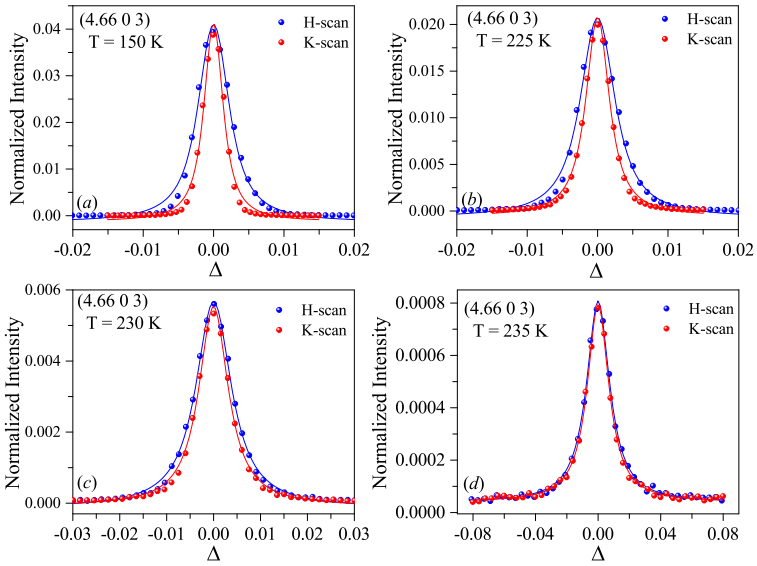

FIG. 5. (Color online) Comparison of the peak profiles along the H- and K-direction at different temperatures. In order to compare the peak profiles along the H- and K-direction, the central positions of the charge stripe reflection (4.66 0 3) are set to zero. (a) Below temperature T ~218 K, the ratio of peak widths along H- and K-directions is almost constant. (b) and (c) Upon warming, the ratio changes as a function of temperature, (d) approaching 1 as the temperature approaches T_{CO} (~238 K).

Figure 5 shows how the peak widths of the charge modulation along the H- and K-directions change as a function of temperature. As can be seen, for temperatures above T_{CO}, the charge modulation is isotropic in the $a \times b$ plane, but as temperature is lowered, there is an anisotropic evolution of the correlation lengths. Figure 6 displays the evolution of the peak profile of charge modulation along c-axis as a function of temperature. As temperature is decreased, the peak narrows at first, indicating an increase in order along

the c-axis, but then it widens again, indicating an inverse order-disorder transition.

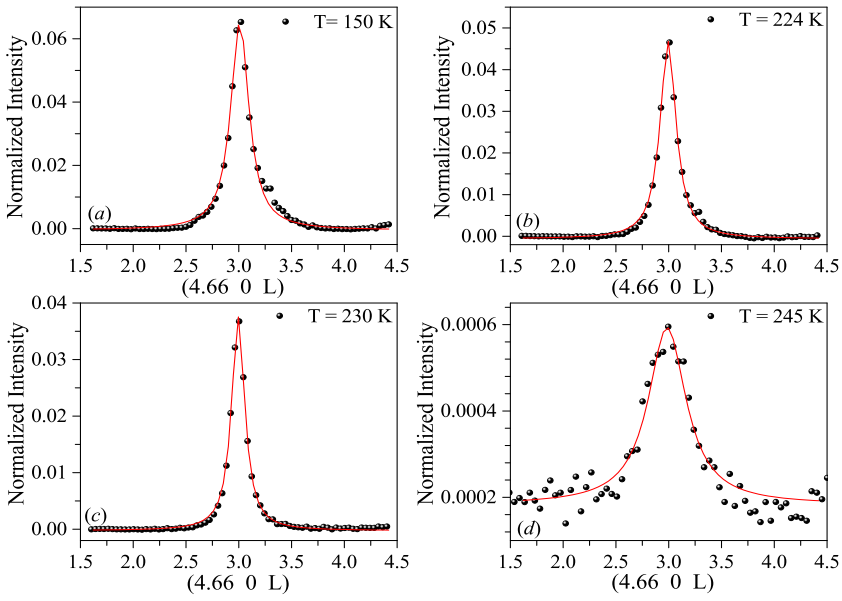

FIG. 6. (Color online) Peak profiles of a charge stripe reflection along the L-direction at different temperatures. Scans through the L-direction (c-axis) of the charge stripe reflection (4.66 0 3) at (a) 150 K, (b) 224 K , (c) 230 K, and (d) 245 K are shown. As temperature is lowered, the peak narrows and becomes sharpest at ∼230 K, but it then widens below 230 K, indicating an inverse order-disorder transition.

For the study of spin stripes, in order to enhance the signals from the spin modulations, a resonant soft x-ray diffraction experiment was conducted on the beamline BL05B3 of NSRRC. The measurements were performed to scan the spin stripe reflection (0.66 0 0) through the L edge of Ni. A large resonance from the spin reflection was observed at the L_3 edge of Ni with incident π-polarized x-rays at T = 80 K. Upon warming, the spin ordering reflection was observed to persist at T = 230 K as shown in figure 7.

APPENDIX: THERMAL HYSTERESIS

Experiments were also conducted to study thermal effects on the charge modulation. The measurement was done on a second crystal of $La_{5/3}Sr_{1/3}NiO_4$. As shown in figure 8, charge stripes show a hysteresis behavior around the transition boundary under different thermal treatments. This is in accordance with previously described thermal phenomena of an electron liquid crystal [34, 35]. The data shown in Figure 8 were collected during

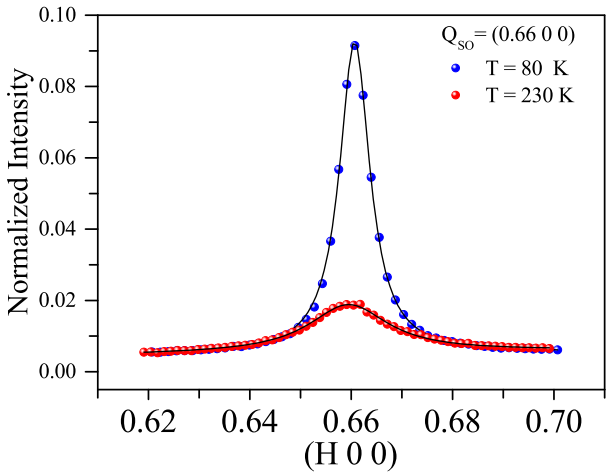

FIG. 7. (Color online) Spin stripe reflection (0.66 0 0) at T = 80 and 230 K. The data were collected by using resonant soft x-ray diffraction at Ni L_3 edge along the a-axis. The black lines are the best fits with a Lorentzian function.

three sequences of warming and cooling. The sample was first cooled down to 130 K from room temperature in approximately 2 hours, and after the alignment at 130 K, the data (as marked by blue triangles in Figure 8) were collected by increasing temperature and scanning the charge stripe reflection (4.66 0 3) along the H, K, and L directions as a function of temperature until T= 250 K, where the reflection becomes very broad and weak. The sample was then warmed up to 260 K and kept at that temperature for approximately half an hour, after which measurements (marked by red dots) were taken as the sample was cooled to T= 140 K. A third round of measurements (marked by open squares) were taken as the sample was warmed up to 250 K once more.

* chd@mail.tku.edu.tw

† yjkao@phys.ntu.edu.tw

[1] P. A. Lee, Naoto Nagaosa, and Xiao-Gang Wen, *Rev. Mod. Phys.* **78** 17-85 (2006)

[2] J. M. Tranquada, B. J.Sternlieb, J. D.Axe, Y.Nakamura andS.Uchida, *Nature* **375**, 561-563 (1995).

[3] G. Ghiringhelli, *et. al.*, *Science* **337**, 821-825 (2012).

[4] J. M. Tranquada, G. D. Gu, M. Hcker, Q. Jie, H.-J. Kang, R. Klingeler, Q. Li, N. Tristan, J. S. Wen, G. Y. Xu, Z. J. Xu, J. Zhou, and M. v. Zimmermann, *Phys. Rev. B* **78**, 174529

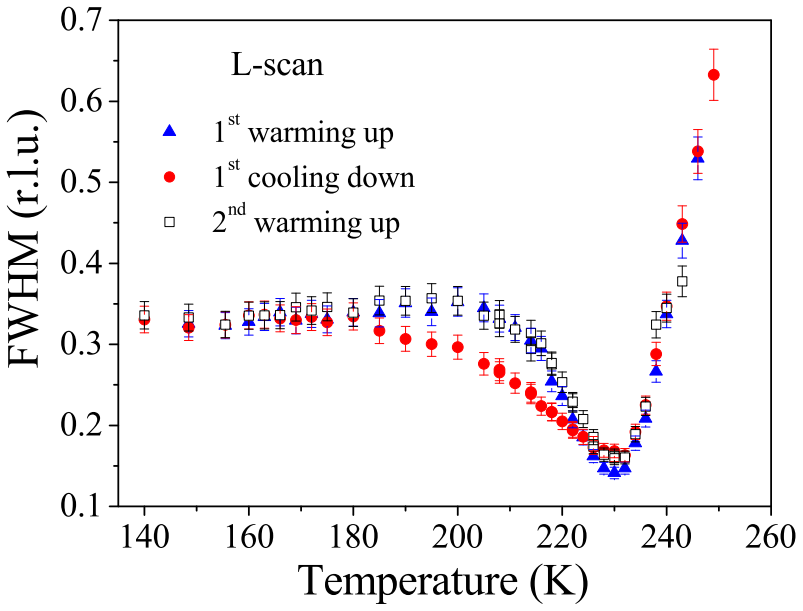

FIG. 8. (Color online) Thermal effects on the charge stripe modulations. Evolution of the peak width (FWHM) of the charge stripe reflection (4.66 0 3) along the L-direction is shown as a function of temperature for the different thermal processes (see the explanation in the supplementary method description). As can be seen, there is some thermal hysteresis.

(2008).

[5] S. A. Kivelson, I. P. Bindloss, E. Fradkin, V. Oganesyan, J.M. Tranquada, A. Kapitulnik and C. Howald, *Rev. Mod. Phys.* **75** 1201-1241 (2003).

[6] E. Fradkin, S. A. Kivelson, M. J. Lawler, J. P. Eisenstein and A. P. Mackenzie, *Annual Review of Condensed Matter Physics* **1**, 153-178 (2010).

[7] S. A. Kivelson, E. Fradkin and V. J. Emery, *Nature* **393**, 550-553

[8] M. Vojta, *Advances in Physics* **58**, 699 (2009).

[9] J. M. Tranquada, H. Woo, T. G. Perring, H. Goka, G. D. Gu, G. Xu, M. Fujita and K. Yamada, *Nature* **429**, 534-538 (2004).

[10] V. Hinkov, D. Haug, B. Fauqu, P. Bourges, Y. Sidis, A. Ivanov, C. Bernhard, C. T. Lin and B. Keimer, *Science* **319**, 597-600 (2008).

[11] R. M. Fernandes, A. V. Chubukov and J. Schmalian, *Nat. Phys.* **10**, 97 (2014).

[12] T.-M. Chuang, M. P. Allan, Jinho Lee, Yang Xie, Ni Ni, S. L. Bud′ko, G. S. Boebinger, P. C. Canfield and J. C. Davis, *Science* **327**, 181-184 (2010).

[13] E. Berg, E. Fradkin, E.-A. Kim, S. A. Kivelson, V. Oganesyan, J. M. Tranquada and S. C. Zhang, *Phys. Rev. Lett.* **99**, 127003 (2007).

[14] W. Hu, S. Kaiser, D. Nicoletti, C. R. Hunt, I. Gierz, M. C. Hoffmann, M. Le Tacon, T. Loew, B. Keimer and A. Cavalleri, *Nature Material* **13**, 705-711 (2014).

[15] P. Freeman, A. T. Boothroyd, D. Prabhakaran, M. Enderle and C. Niedermayer, *Phys. Rev. B*, **70**, 024413 (2004).

[16] S. H. Lee, and S-W. Cheong, *Phys. Rev. Lett.* **79**, 2514-2517 (1997).

[17] S. Anissimova, D. Parshall, G.D. Gu, K. Marty, M.D. Lumsden, Songxue Chi, J.A. Fernandez-Baca, D.L. Abernathy, D. Lamago, J.M. Tranquada and D. Reznik, *Nat. Commun.* **5**, 3467 (2014).

[18] S. H. Lee, J. M. Tranquada, K. Yamada, D. J. Buttrey, Q. Li and S.-W. Cheong, *Phys. Rev. Lett.* **88**, 126401 (2002).

[19] R. J. Cava, B. Batlogg, T. T. Palstra, J. J. Krajewski, W. F. Peck, A. P. Ramirez and L. W. Rupp, *Phys. Rev. B* **43** 1229-1232 (1991).

[20] A. M. M. Abeykoon, E. S. Božin, Wei-Guo Yin, Genda Gu, John P. Hill, John M. Tranquada and Simon J. L. Billinge,, *Phys. Rev. Lett.* **111**, 096404 (2013).

[21] M. Hücker, M. v. Zimmermann and G. D. Gu, *Phys. Rev. B* **74** 85112 (2006).

[22] C.-H. Du, M. E. Ghazi, Y. Su, I. Pape, P. D. Hatton, S. D. Brown, W. G. Stirling, M. J. Cooper and S-W. Cheong, *Phys. Rev. Lett.* **84**, 3911 (2000).

[23] O. Zachar, S. A. Kivelson and V. J. Emery, *Phys. Rev. B* **57**, 1422-1426 (1998).

[24] E. P. Rosenthal, E. F. Andrade, C. J. Arguello, R. M. Fernandes, L. Y. Xing, X. C. Wang, C. Q. Jin, A. J. Millis and A. N. Pasupathy, *Nat. Phys.* **10**, 225-232 (2014).

[25] A. P. Ramirez, P. L. Gammel, S-W. Cheong, D. J. Bishop, and P. Chandra, *Phys. Rev. Lett.* **76**, 447-450 (1996).

[26] R. Kajimoto, T. Kakeshita, H. Yoshizawa, T. Tanabe, T. Katsufuji, and Y. Tokura, *Phys. Rev. B* **64**, 14432 (2001).

[27] R. Yoshizawa, T. Kakeshita, R. Kajimoto, T. Tanabe, T. Katsufuji, and Y. Tokura, *Phys. Rev. B* **61**, 854-857 (2000).

[28] K. Ishizaka, T. Arima, Y. Murakami, R. Kajimoto, H. Yoshizawa, N. Nagaosa, and Y. Tokura,, *Phys. Rev. Lett.* **92**, 196404 (2004).

[29] J. Li, Y. Zhu, J. M. Tranquada, K. Yamada, and D. J. Buttrey, *Phys. Rev. B* **67**, 012404 (2003).

[30] J. Lloyd-Hughes, D. Prabhakaran, A. T. Boothroyd, and M. B. Johnston, *Phys. Rev. B* **77**, 195114 (2008).

[31] W. S. Lee, *et al.*, *Nat. Commun.* **3**, 383 (2012).

[32] A. T. Boothroyd, P. Babkevich, D. Prabhakaran and P. G. Freeman, *Nature* **471**, 341-344 (2011).

[33] T. Lancaster, S. R. Giblin, G. Allodi, S. Bordignon, M. Mazzani, R. De Renzi, P. G. Freeman, P. J. Baker, F. L. Pratt, P. Babkevich, S. J. Blundell, A. T. Boothroyd, J. S. Mller, and D. Prabhakaran, *Phys. Rev. B* **89**, 020405 (2014).

[34] E. W. Carlson, and K. A. Dahmen, *Nat. Commun.* **2**, 379 (2010).

[35] Cheol Eui Lee, and S. H. Yang, *J. of the Korean Phys. Soci.* **33**, L635-L637 (1998).